

## Research Article

# Antibacterial Shoe Insole-Coated CuO-ZnO Nanocomposite Synthesized by the Sol-Gel Technique

Nguyen Lam Uyen Vo,<sup>1,2</sup> Thi Thuy Van Nguyen,<sup>3,4</sup> Tri Nguyen ,<sup>3,5</sup> Phung Anh Nguyen,<sup>3</sup> Van Minh Nguyen,<sup>5</sup> Ngoc Huy Nguyen,<sup>1,2</sup> Van Linh Tran,<sup>1,2</sup> Ngoc Anh Phan,<sup>1,2</sup> and Ky Phuong Ha Huynh <sup>1,2</sup>

<sup>1</sup>Vietnam National University Ho Chi Minh City, Linh Trung Ward, Thu Duc District, Ho Chi Minh City, Vietnam

<sup>2</sup>Ho Chi Minh City University of Technology (HCMUT), 268 Ly Thuong Kiet Street, Ho Chi Minh City, Vietnam

<sup>3</sup>Institute of Chemical Technology, Vietnam Academy of Science and Technology, Ho Chi Minh City, Vietnam

<sup>4</sup>Graduate University of Science and Technology, Vietnam Academy of Science and Technology, Hanoi, Vietnam

<sup>5</sup>Biotechnology Department, Ho Chi Minh City Open University, Ho Chi Minh City, Vietnam

Correspondence should be addressed to Ky Phuong Ha Huynh; [hkpha@hcmut.edu.vn](mailto:hkpha@hcmut.edu.vn)

Received 28 September 2020; Revised 23 November 2020; Accepted 8 December 2020; Published 17 December 2020

Academic Editor: Duy Trinh Nguyen

Copyright © 2020 Nguyen Lam Uyen Vo et al. This is an open access article distributed under the Creative Commons Attribution License, which permits unrestricted use, distribution, and reproduction in any medium, provided the original work is properly cited.

In this study, CuO-ZnO composite was synthesized via the sol-gel method using oxalic acid to form the medium complex and its applications in antibacterial have been conducted with *B. cereus*, *E. coli*, *S. aureus*, *Salmonella*, and *P. aeruginosa*. Then, nanopowder of CuO-ZnO was coated on shoe insoles and their antibacterial effect with *S. aureus* was tested. The nanocomposite products were characterized by XRD, XPS, SEM, TEM, and UV-Vis. The results showed that the CuO-ZnO composite has the average particle size in a range of 20-50 nm, the point of zero charge of 7.8, and the bandgap of 1.7 eV. XPS result shows the composite structure with Cu<sup>2+</sup> in the product. The minimum inhibitory concentration (MIC) of CuO-ZnO nanocomposite was 0.313 mg·mL<sup>-1</sup> for *S. aureus* and *Samonella*, 0.625 mg·mL<sup>-1</sup> for *E. coli*, and 5 mg·mL<sup>-1</sup> for *B. cereus* and *P. aeruginosa*. The shoe insoles coated with 0.35 wt.% of CuO-ZnO nanocomposite also had high antibacterial activity against *S. aureus*, and this antibacterial nanocomposite was implanted durably on the surface of the shoe insoles.

## 1. Introduction

Nowadays, the increasing of food and habitat that leads to the increasing of various microorganisms is observed throughout the globe. Microbial pollution is a big problem of the environment, water sources, and public health. Besides, the development of drug resistance and the emerging infectious diseases in the pathogenic bacteria and fungi at an alarming rate is a matter of serious concern. Although modern therapeutics and microbial pathogenesis are developed fast, the morbidity associated with microbial infections is still very high, especially in rural areas [1]. Furthermore, microbial contamination effects are highly estimated in the healthcare and food industry. In recent decades, antimicrobial agents and surface coating have been studied widely. Recently, the

applications of nanotechnology in medicine have contributed to a new field of technology and bring significant advances in the fight against various diseases [2]. Many new studies show that nanoantibacterial materials can be applied in various fields with high antibacterial efficiency and low content [3]. There are some new nanomaterials that were introduced with a high antibacterial ability such as Ag [4, 5], Cu [5, 6], ZnO [7–9], TiO<sub>2</sub> [10], Au [11], or CeO<sub>2</sub> [12]. Their antibacterial efficiency depends on the shape, size of particles, and also chemical compositions and concentration [13]. As one of nanoantibacterial materials, ZnO shows its essential role in healthcare products, UV blocking capability, biocompatibility, and low cost [14]. Nanoparticles of ZnO can be used as a multifunctional inorganic compound with powerful antibacterial action. With low concentration, zinc oxide

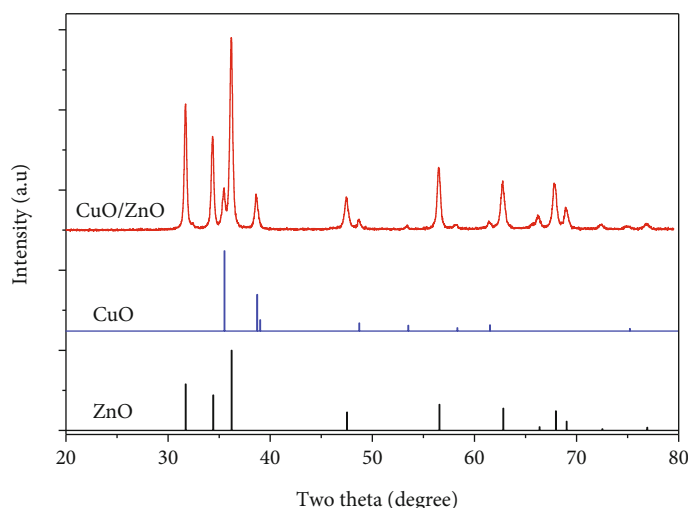


FIGURE 1: XRD pattern of CuO-ZnO composite.

nanoparticles also show their antibacterial and antifungal activities and the antifungal activity does not influence soil fertility as some conventional antifungal agents [15]. Besides, the electronic, magnetic, optical, and electrical characterization of ZnO can be changed and be useful for various practical applications; some transition metals (Cu, Ni, Co, Pd, Au, and Ag) are doped in its structure [16–19]. Compared to pure ZnO, metal- or metal oxide-doped ZnO demonstrates a greater effect against pathogenic organisms in this method using nanoparticle material as an antimicrobial agent and is considered one of the most useful techniques to minimize the cost and chemical waste [20]. Besides, the combination of two or more metallic components with metal oxides includes the elaboration of nanostructured oxides that increased their potential applications due to their unique electronic, optical, magnetic, and other physicochemical properties [21].

Copper has been shown to have a good antibacterial property by Fenton reactions [22–25]. But copper is relatively expensive and has a dark color lead to less aesthetic in applications, while colorless ZnO should be easier to apply in practice. Therefore, copper doped with a small amount into the ZnO structure will enhance the antibacterial property of the material while not darkening the material [16, 22, 25, 26]. The potent antibacterial properties of ZnO/CuO nanocomposite may be attributed to the released metal ions, which could have interaction with bacteria by means of their attaching to the surface of the cell membranes of bacteria and penetrating into the bacterial cells. The authors [27–30] also had similar explanations by observing SEM images of bacteria before and after treatment with zinc and copper oxide.

However, there are very few works that compare the antibacterial activity of many different bacterial strains to ZnO and CuO-ZnO nanomaterials as well as their applications are also limited. The use of CuO-ZnO nanomaterial in shoe insoles has not been announced previously. In fact, shoe insoles are susceptible to infection, which can harm human health and create bad odors. Weng et al. synthesized copper-coated insoles to inhibit foot-odor-producing bacte-

ria targeting *Staphylococcus* species. The results indicated that the efficacy of copper is against the growth of bacteria [31]. Yip et al. [32] synthesized selenium nanoparticles padded onto the fabric of shoe insoles to obtain antifungal and antibacterial fabric. It was found that the fabric of insoles treated with selenium nanoparticles can inhibit the development of *Staphylococcus* effectively in the first 12 h. The shoe insoles coated with a very low concentration of CuO-ZnO were expected to have good antimicrobial resistance.

In this study, CuO-ZnO composite will be synthesized using the sol-gel method and the antibacterial activity of CuO-ZnO composite as well as pure ZnO will be tested with five different bacteria *B. cereus*, *E. coli*, *S. aureus*, *Salmonella*, and *P. aeruginosa*. According to previous studies [33, 34], *S. aureus* was described as microbiota associated with feet skin. When exposed to favorable environments with high humidity such as shoe soles, they easily multiply and grow. Therefore, in this study, CuO-ZnO with low concentration will be then impregnated on the shoe insoles and antibacterial activity with *S. aureus* under different conditions to prove the real usage applicability is investigated.

## 2. Experimental

**2.1. Synthesis of Materials.** CuO-ZnO nanocomposite with the CuO/ZnO mole ratio of 1:4 was synthesized by dissolving 23.76 grams of  $\text{Zn}(\text{NO}_3)_2 \cdot 6\text{H}_2\text{O}$  (Xilong, >99%) into 50 mL distilled water; then, 37.80 grams of oxalic acid (Merck, >99%) was added. The mixture was vigorously mixed using a magnetic stirrer and heated up to 80°C for 2 hours until the solution is transparent. After that, the solution prepared from 11 mL of ethylene glycol (Xilong, >99.8%) and 4.84 grams of  $\text{Cu}(\text{NO}_3)_2 \cdot 3\text{H}_2\text{O}$  (Xilong, >99%) was dropped into the previous solution; then, the solution was added with distilled water to reach 100 mL totally, during stirring continuously all the time, and the solution with light blue color was obtained. After 2 hours under 80°C conditions, the solution was changed to a gel state and then reach the past state when the temperature was increased. The gel mixture was dried at 200°C within 2 hours and then calcined

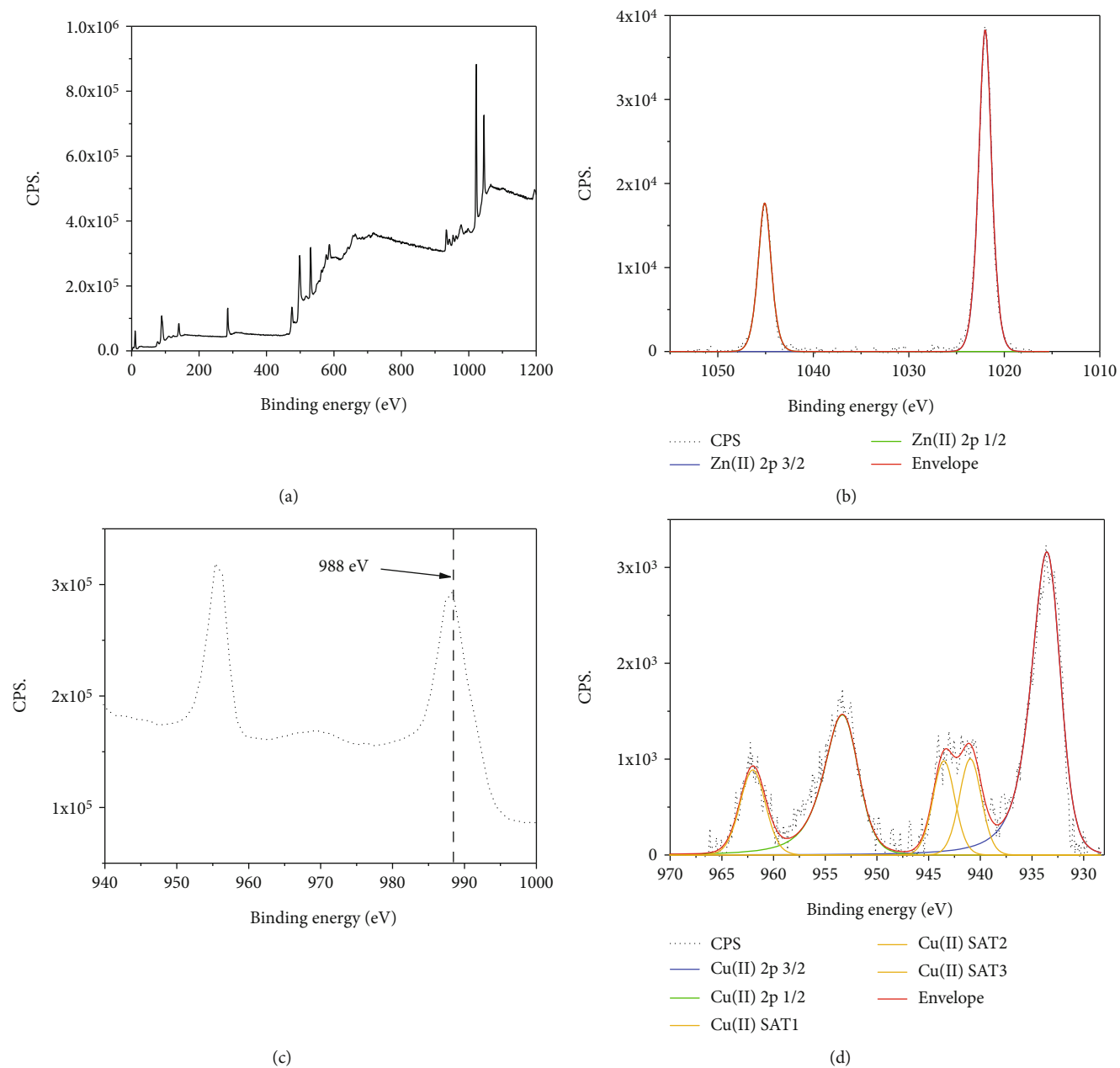


FIGURE 2: Continued.

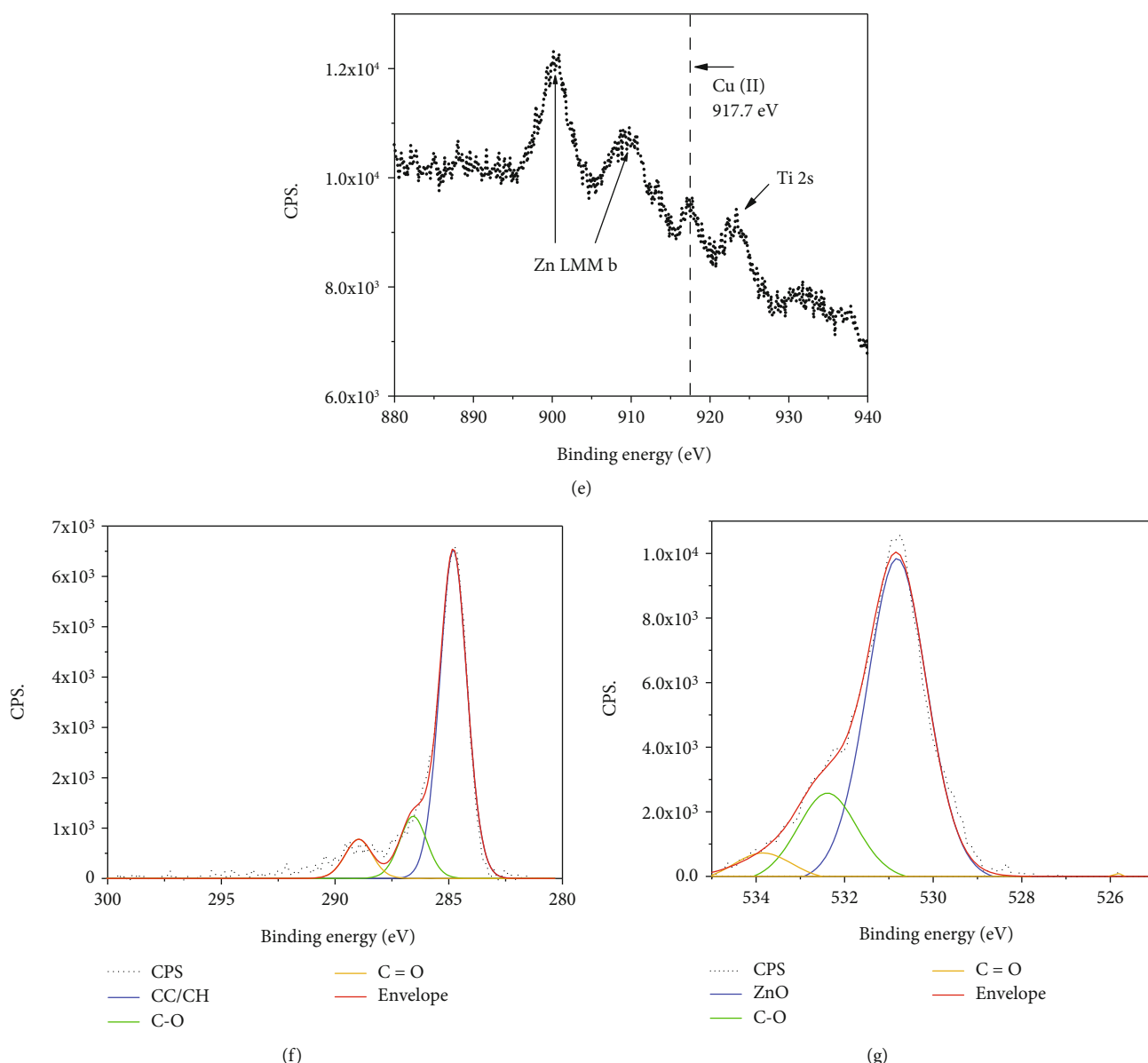


FIGURE 2: The survey spectrum XPS spectrum (a) and Zn 2p (b), Zn LMM auger region (c), Cu 2p (d), Cu LMM auger region (e), C 1s (f), and O 1s (g) core level high-resolution XPS spectra of CuO-doped ZnO sample.

at  $500^\circ\text{C}$  for 2 hours in the airflow with a flow rate of  $3 \text{ L}\cdot\text{h}^{-1}$  with a heating rate of  $10^\circ\text{C}\cdot\text{min}^{-1}$  to obtain CuO-ZnO nanocomposite. This powder was ball ground in 12 hours, and the nanocomposite powder of product was obtained for antibacterial activity testing and other physicochemical characteristic analyses. In the synthesis of this work, by the sol-gel method, oxalic acid was used to form the medium complex compounds with  $\text{Zn}^{2+}$  and  $\text{Cu}^{2+}$ , where ethylene glycol was used as a dispersing agent. Then, after being dried at  $200^\circ\text{C}$  to remove all free water as well as ethylene glycol, the mixture powder that consisted of metallic organic compounds will have a much lower calcination temperature ( $500^\circ\text{C}$ ) to form CuO-ZnO compared to other methods [35, 36].

To synthesize nanopowder ZnO as a control sample, the same process to the previous was also performed without the solution of  $\text{Cu}(\text{NO}_3)_2\cdot 3\text{H}_2\text{O}$  in ethylene glycol.

**2.2. Preparation of Antibacterial Shoe Insole-Coated CuO-ZnO Nanocomposite.** The antibacterial shoe insole-coated CuO-ZnO nanocomposite was prepared as follows: 2 grams of CuO-ZnO nanoparticles were dispersed in 50 mL of the solution of 2 wt.% of the cloth starching in the distilled water at  $80^\circ\text{C}$  and 2 hours. Next, the samples of shoe insoles with the size of  $2 \text{ cm} \times 2 \text{ cm}$  were dipped into this solution. The antibacterial shoe insoles were obtained after drying at  $80^\circ\text{C}$  in 24 hrs. The CuO-ZnO amount coated on the surface of shoe insoles was fixed at 0.35 wt.% (CuZn/S-1 sample).

To evaluate the durability of antibacterial materials on the surface, 02 samples washed under two different conditions are tested: the first sample washed and rubbed with a soap solution (the weight ratio of soap/water at 1/5) for 15 minutes, and then drying at  $80^\circ\text{C}$  in 24 hrs (CuZn/S-2 sample); another sample only soaked in the soap solution (not

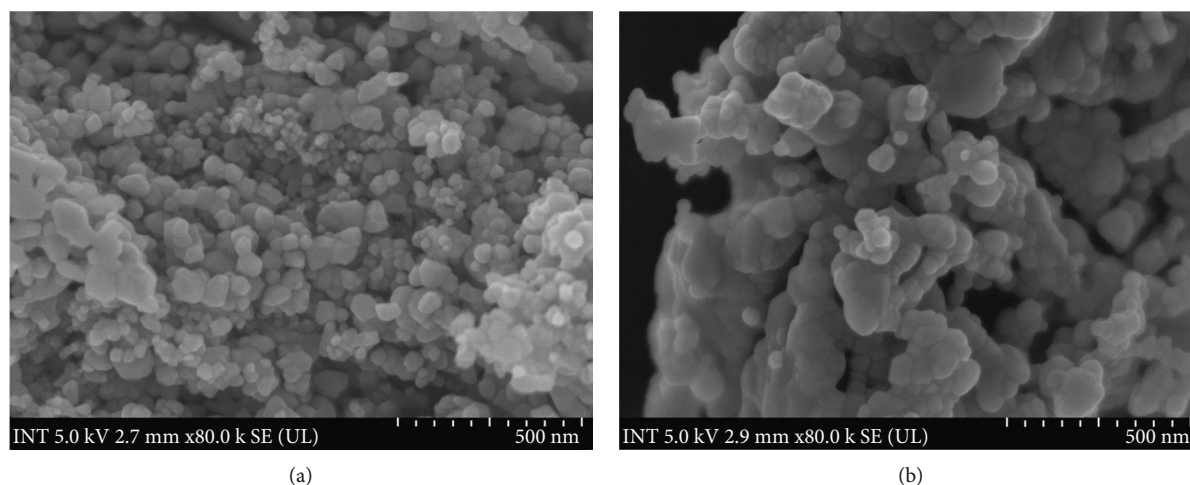


FIGURE 3: SEM images of ZnO (a) and CuO-ZnO (b).

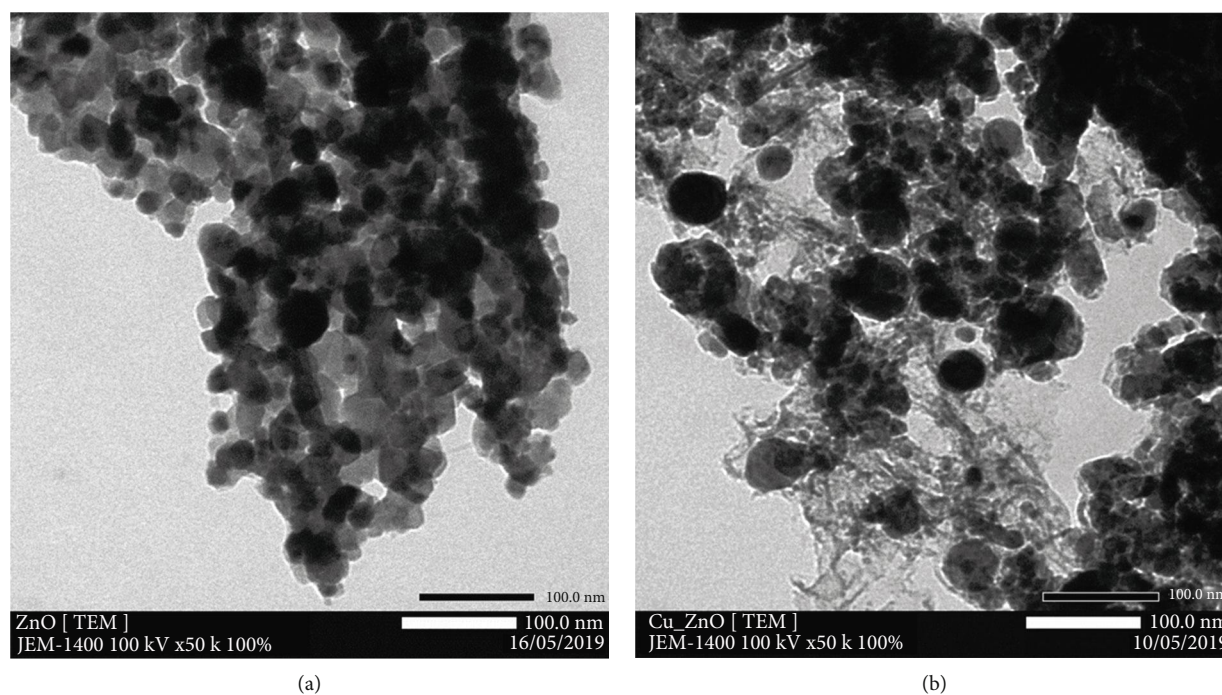


FIGURE 4: TEM images of ZnO (a) and CuO-ZnO (b).

rubbed) for 24 hours and then cleaning by the distilled water and drying at the same conditions (CuZn/S-3 sample). And, a sample which was not coated with CuO-ZnO nanoparticles was used as a control.

**2.3. Characterization of Samples.** Both nanopowders of pure ZnO and CuO-ZnO composite were investigated according to their structure using X-ray Diffraction (XRD) on a Bruker D2 Phaser diffractometer using  $\text{CuK}\alpha$  radiation ( $\lambda = 0.154$  nm) in  $2\theta = 10 - 80^\circ$  with the scanning step of  $0.02^\circ$ . Nitrogen adsorption and desorption isotherms were measured on the Nova 2200e Instrument at  $-196^\circ\text{C}$ . The morphology of samples was characterized by scanning electron microscopy (SEM) on the Hitachi S4800 instrument. The morphology, particle size, and crystal phases were also estimated by

transmission electron microscopy analysis (TEM) on the JEOL JEM 1400 instrument. Samples were analyzed by X-ray photoelectron spectroscopy analysis (XPS) using a Kratos SUPRA XPS fitted with a monochromated  $\text{Al K}\alpha$  X-ray source (1486.69 eV) (high tension: 15 kV, emission current 10 mA) and an electron flood gun charge neutralizer. Samples were affixed to stage using carbon tape to attach samples to a microscope slide to ensure full electrical isolation from the system. Samples entered the analysis chamber at a pressure below  $1 \times 10^{-8}$  Torr. Survey scans were recorded at a pass energy of 160 eV. High-resolution spectra were recorded using a pass energy of 40 eV using a hybrid lens mode and a slot aperture. The point of zero charge (PZC) of samples was determined by the salt addition method [37]. The UV-Vis diffuse reflectance spectroscopy (DRS) was used to examine



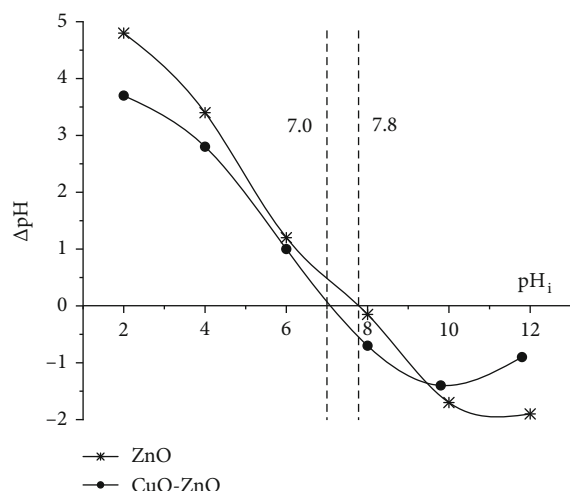


FIGURE 5: Isoelectric pH of ZnO nanoparticles and CuO-ZnO nanoparticles.

the bandgap of the samples and recorded on a Varian Cary 5000 UV-Vis-NIR spectrophotometer with an integrating sphere in the range of 200–800 nm.

The shoe insole-coated CuO-ZnO nanocomposite has characterized the morphology by scanning electron microscopy (SEM), EDS mapping, and EDX spectrum on the JEOL JST-IT 200 instrument.

**2.4. Testing Antibacterial Activity of Samples.** The obtained nanopowder ZnO and Cu-doped ZnO samples were used to test for antibacterial activities against *B. cereus* (ATCC 14579), *E. coli* (ATCC 25922), *S. aureus* (ATCC 43300), *Salmonella typhi* (ATCC 14028), and *P. aeruginosa* (ATCC 15442). To examine the MIC of CuO-ZnO and ZnO against these five bacteria, different concentration solutions of samples ( $N$ ,  $N/2$ ,  $N/4$ ,  $N/8$ ,  $N/16$ ,  $N/32$ ,  $N/64$ , and  $N/128$  with  $N$  was the initial concentration of the solution,  $N = 20 \text{ mg} \cdot \text{mL}^{-1}$ ) in deionized water were prepared. Subsequently, the diluted samples were mixed with the sterile nutrient agar. By using sterile sticks, the standardized inoculum of each selected bacteria with  $1.5 \times 10^7 \text{ CFU} \cdot \text{mL}^{-1}$  was inoculated on agar plates mixed with samples from low to high concentrations. One plate of the sterile nutrient agar was not mixed with the sample as a control [38]. Each strain of bacteria was inoculated at one point on a plate with the same location on the plates. Finally, the plates were incubated at  $37^\circ\text{C}$  for 24 hours. The lowest concentration of samples that inhibits the growth of tested bacteria was considered as the minimum inhibitory concentration (MIC) [39].

For the shoe insole-coated CuO-ZnO nanocomposite, a sample piece was put in Petri plates in a UV stove ( $\lambda = 254 \text{ nm}$ ) within 2 hours to kill all bacteria.  $50 \mu\text{L}$  of prepared bacteria solution was filled in a plate where the nutrient agar slant was previously prepared in the area of the sample. The sample was put into the prepared agar plate at the position where the sample surface was in contact with the surface of a nutrient agar plate. The plate was preserved at  $37^\circ\text{C}$  for 24 hours. The sample uncoated

CuO-ZnO nanocomposite was used as a control. The antibacterial activity of samples was evaluated by the levels of bacteria colonies not detected on the surface samples.

### 3. Results and Discussion

**3.1. Characteristics of Materials.** As seen in Figure 1, the sharp diffraction peaks obtained from the ZnO sample at  $2\theta = 31.8^\circ, 34.4^\circ, 36.3^\circ, 47.5^\circ, 56.6^\circ, 62.9^\circ, 66.4^\circ$ , and  $69.0^\circ$  illustrated a good crystallinity structure and high purity [16, 40]. These peaks correspond to the lattice planes (100), (002), (101), (110), (103), (112), (201), and (200) indexed to the hexagonal wurtzite structure. For the CuO-ZnO sample, apart from the same peaks identified in the ZnO samples, four new diffraction peaks were observed at  $35.5^\circ, 38.7^\circ, 48.7^\circ, 53.5^\circ, 58.3^\circ, 61.5^\circ$ , and  $75.2^\circ$  which are the characteristic peaks of CuO (JCPDS card No. 05-0661).

The average crystal size of CuO at  $2\theta = 35.5^\circ$  and ZnO at  $2\theta = 36.3^\circ$  was calculated according to the Scherrer equation [41]:

$$d(\text{nm}) = \frac{K\lambda}{\beta \cos \theta}, \quad (1)$$

where  $K$ , the Scherrer constant, is taken to be 0.94,  $\lambda$  is the wavelength of the X-ray,  $\beta$  is the line width at half maximum height of the peak in radians, and  $\theta$  is the position of the peak in radians. By Scherrer's equation, the average crystallite size of ZnO in a pure ZnO sample is determined to be 19.1 nm compared to 27.0 nm for the ZnO-CuO sample. And the average crystallite size of CuO in the ZnO-CuO sample is 25 nm. It can be explained due to the incorporation of CuO as a dopant compound on the surface of the ZnO matrix then leads to increasing of crystal size [42, 43]. This result is lower than other results [44–46] which were synthesized by the sol-gel method (50–100 nm). The material has a small and uniform particle size maybe because the calcined temperature of the medium complex compound which was obtained after drying is much lower than that of the sol-gel method; then, the agglomeration during the calcination process is limited. It was proved that materials which have smaller particle size also have better antibacterial properties [47, 48].

Shown in Figure 2 is the evidence of the formation of the CuO, ZnO, and ZnO/CuO nanostructures. The high-resolution XPS spectrum of Zn 2p for the pure ZnO and that of CuO was observed. Zn appeared to be in the form of purely  $\text{Zn}^{2+}$  (binding energy of 1022 eV in Figure 2(b)), which is further supported by the presence of the  $\text{Zn}2p_{1/2}$  and  $\text{Zn}2p_{3/2}$  peaks observed at 1045.1 and 1022 eV, respectively [49]. That means, the bonding energy difference between these two peaks is 23.1 eV, which is further supported by the presence of a single peak within the Zn LMM auger region centered at 988 eV (Figure 2(c)). Figures 2(d) and 2(e) showed that Cu appears to be in the form of purely  $\text{Cu}^{2+}$ . There are two peaks at 933.95 and 953.7 eV that correspond to the Cu  $2p_{3/2}$  and Cu  $2p_{1/2}$ , respectively [50]. Therefore, the bonding energy difference between these two peaks is 19.75 eV (Figure 2(d)). Besides, there are two satellite peaks centered around 944

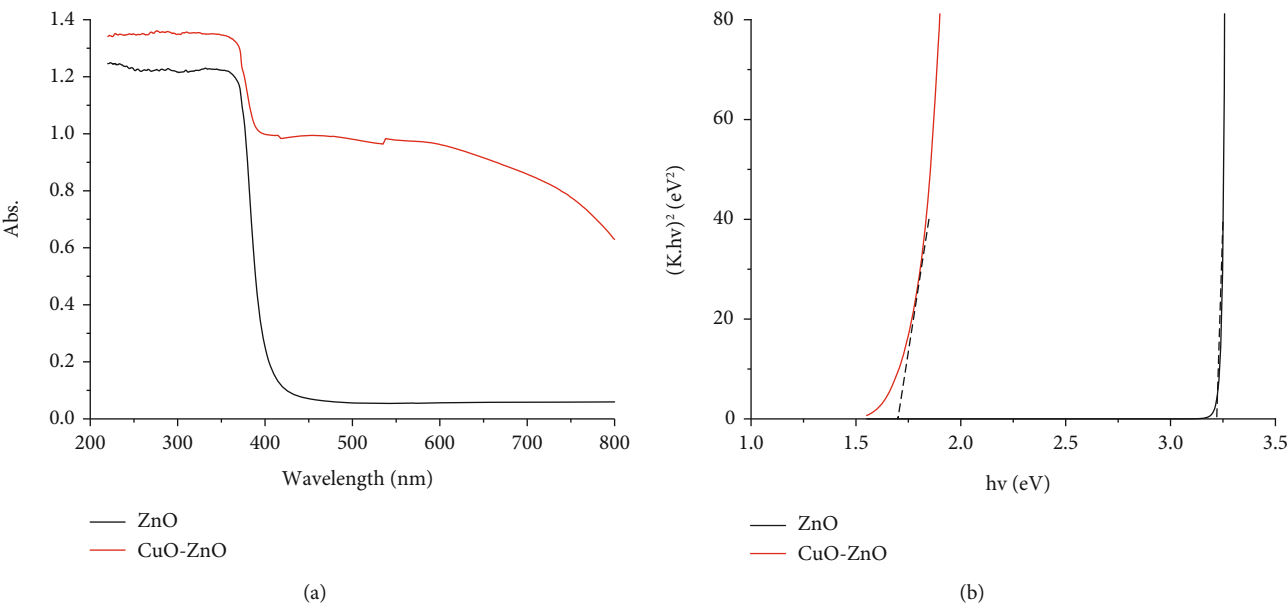


FIGURE 6: UV-Vis spectra (a) and Tauc's plot (b) of ZnO and CuO-ZnO samples.

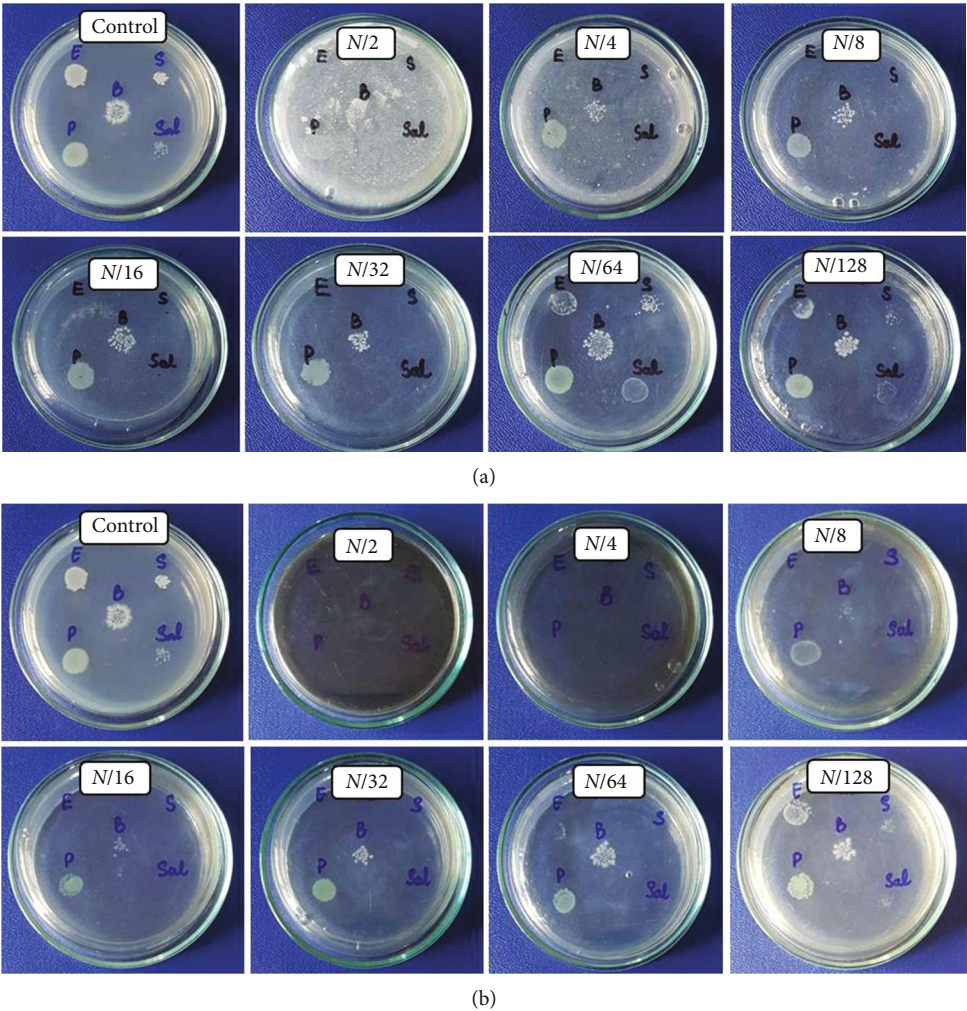


FIGURE 7: The minimum inhibitory concentrations of pure ZnO (a) and CuO-ZnO composite (b) against *E. coli* (E), *B. cereus* (B), *S. aureus* (S), *Salmonella* (Sal), and *P. aeruginosa* (P).

TABLE 1: The comparison of minimum inhibitory concentrations of ZnO and Cu-ZnO samples against five bacteria.

Concentrations of sample	<i>E. coli</i>		<i>B. cereus</i>		<i>S. aureus</i>		<i>Salmonella</i>		<i>P. aeruginosa</i>	
	ZnO	Cu-ZnO	ZnO	Cu-ZnO	ZnO	Cu-ZnO	ZnO	Cu-ZnO	ZnO	Cu-ZnO
N	+	+	+	+	+	+	+	+	-	+
N/2	+	+	-	+	+	+	+	+	-	+
N/4	+	+	-	+	+	+	+	+	-	+
N/8	+	+	-	-	+	+	-	+	-	-
N/16	+	+	-	-	+	+	-	+	-	-
N/32	+	+	-	-	+	+	-	+	-	-
N/64	-	-	-	-	-	+	-	+	-	-
N/128	-	-	-	-	-	-	-	-	-	-

N = 20 mg·mL<sup>-1</sup>; +: antibacterial; -: no antibacterial.

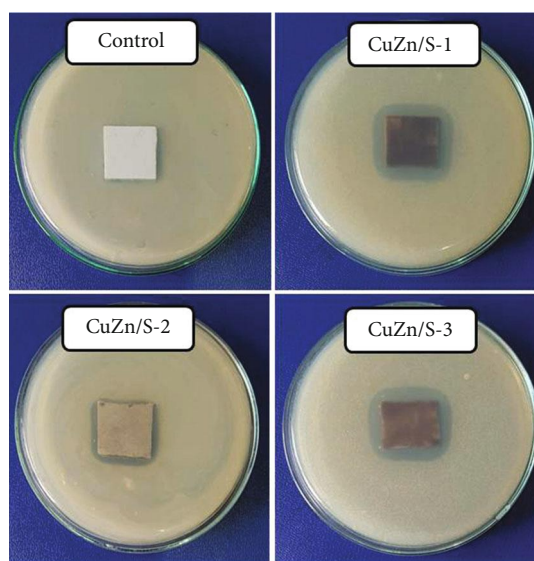


FIGURE 8: Antibacterial activity of shoe insole-coated CuO-ZnO nanocomposite against *S. aureus*.

and 962 eV, which present the bivalence oxidation state of Cu [51]. This is also supported by the single peak within Cu LMM centered around 943 eV (Figure 2(e)). The Cu LMM region, furthermore, is very tricky to analyze due to the presence of Zn LMM and Ti 2s photoelectron peaks in the near vicinity, though it can be determined with some certainty that neither Cu<sup>+</sup> nor Cu<sup>0</sup> appears to be present. In Figure 2(g), the O 1s XPS spectra of the CuO/ZnO composite in terms of binding energy are presented.

Figure 3(a) shows that ZnO had uniform spherical particles from 10 to 30 nm, which was smaller than the ZnO sample obtained from Nigussie et al.'s work [16]. For CuO-ZnO composite (Figure 3(b)), the nanoparticle size was in a range of 20–50 nm connected to form clusters. TEM images (Figure 4) also show that the size of CuO-ZnO nanoparticles is larger than that of ZnO. It is possible that CuO and ZnO crystals bind together to form large particles or cluster (also seen in the SEM figure). The average size of ZnO nanoparti-

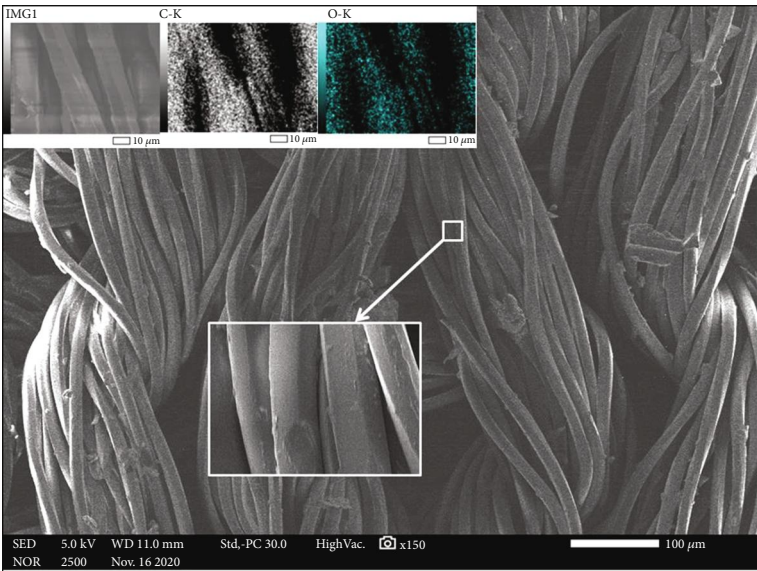
cles synthesized by the sol-gel method in this work is 20 nm, being equal to that of the ZnO sample synthesized by a microwave-assisted combustion method [52]. These results are also compatible with the calculation results base on XRD patterns using Scherrer's equation.

The addition of CuO decreased the PZC of composite (Figure 5). ZnO material has PZC of 7.8, and this value will be decreased to 7.0 when CuO is added; this leads to the increasing of positive ions on CuO-ZnO material and then increasing also its antibacterial ability [53].

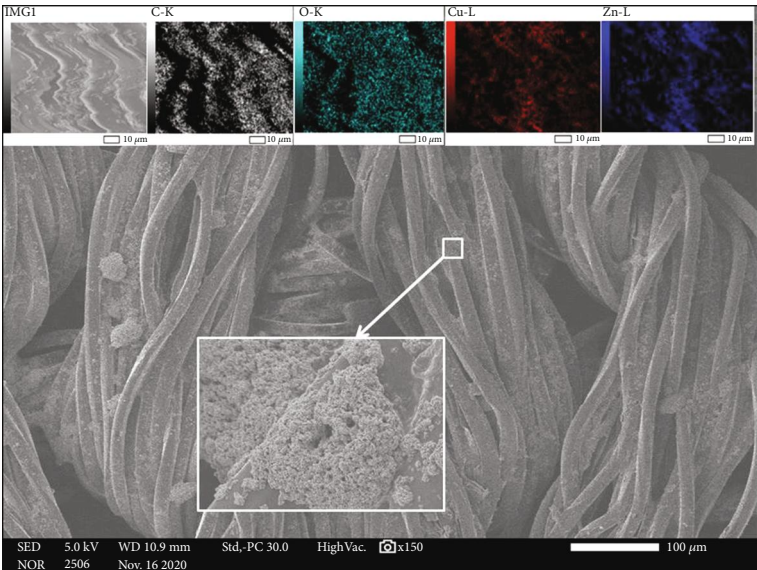
Figure 6 show that the bandgap of ZnO and CuO-ZnO is 3.2 eV and 1.7 eV, respectively. This result proved that the bandgap of composite will be reduced when CuO is doped into ZnO. It can be explained that the increasing of bandgap due to the combination transition enhanced from O<sub>2</sub> (2p) to Zn<sup>2+</sup> (3d<sup>10</sup>–4s) and to Cu<sup>2+</sup> (3d<sup>9</sup>). The reducing of bandgap in composite material leads to enhancing the radical species such as ·O<sub>2</sub><sup>-</sup>, HO<sub>2</sub><sup>·</sup>, and HO<sub>2</sub><sup>-</sup> [54].

**3.2. Antibacterial Activity of Samples.** The results from Figure 7 and Table 1 show the effect of ZnO nanoparticles to bacteria by the decreasing antibacterial activity of *E. coli*~*S. aureus* (0.625 mg·mL<sup>-1</sup>)>*Samonella* (5 mg·mL<sup>-1</sup>)>*B. cereus* (20 mg·mL<sup>-1</sup>)>*P. aeruginosa* (>20 mg·mL<sup>-1</sup>), while the result of CuO-ZnO to bacteria is *S. aureus*~*Samonella* (0.313 mg·mL<sup>-1</sup>)>*E. coli* (0.625 mg·mL<sup>-1</sup>)>*B. cereus*~*P. aeruginosa* (5 mg·mL<sup>-1</sup>). This result also shows that *E. coli* is sensitive for ZnO, but it is less sensitive for CuO than *S. aureus*. It can be explained that bacteria rich in amine and carboxyl groups at the surface, like *S. aureus*, bind stronger CuO then is more sensitive to its bacterial property [25, 55, 56]. At the same time, the results have shown that the antibacterial of CuO-ZnO is increased against *E. coli*, *B. cereus*, *S. aureus*, *Salmonella*, and *P. aeruginosa* strains, as revealed by 4 times, 2 times, 16 times, and higher 4 times of the MIC value than pure ZnO. These results clearly show that the role of CuO in nanocomposite affects antibacterial properties. The inhibition and destruction of bacterial cells are explained by many different mechanisms. For nanoparticles, the antibacterial mechanism is mainly based on the mechanism of nanocell poisoning, most of known antibacterial nanomaterials releasing of positive ion that interacts electrostatically with the bacterial membrane causing disruption of the membrane, or



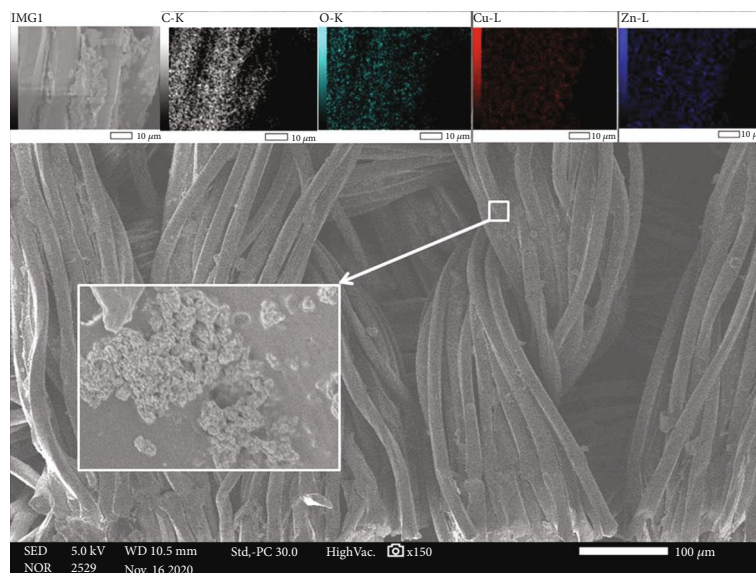


(a)

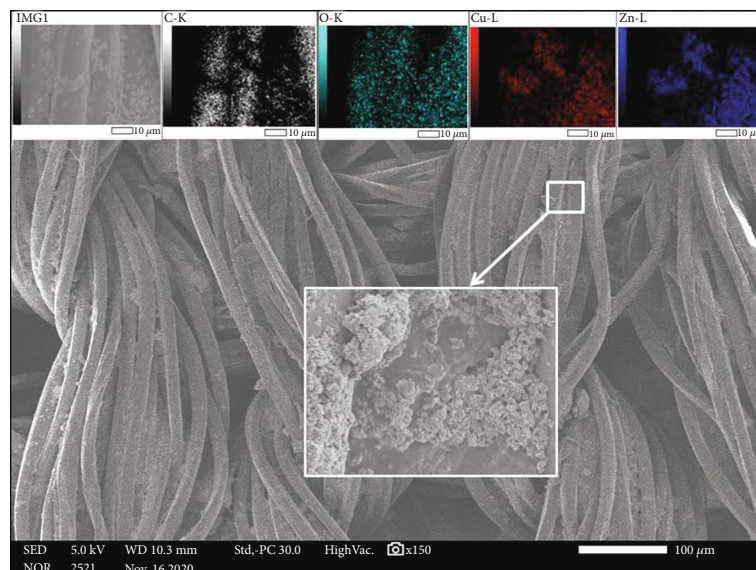


(b)

FIGURE 9: Continued.



(c)



(d)

FIGURE 9: SEM images and EDS mappings of the shoe insole-coated CuO-ZnO nanocomposite: (a) the control sample (the fresh shoe insoles), (b) CuZn/S-1, (c) CuZn/S-2, and (d) CuZn/S-3.

disturbance of permeability [43, 57, 58]. There are some previous publishes that show the generation of reactive oxidation species (ROS), which can destroy the secondary membranes, hinder the function of proteins, and destroy DNA [59, 60]. Or some other studies proved that photoactivated antibacterial nanoparticles have strong oxidation properties that can destroy the outer membranes of bacteria and cause bacterial death [61, 62]. When two or more oxides of antibacterial material are combined to make nanocomposite, they can produce a larger amount of ROS, which leads to enhancing the antibacterial property of composite materials. Actually, ROS can also be produced in the conditions that there is no light irradiation according to many previous studies [63, 64]. Besides, the bandgap energy results in Figure 6(b) showed the decreasing bandgap of CuO-ZnO compared to

ZnO that proved the ability to produce easier ROS from materials. Besides, the surface charge was also shown to play an important role in membrane damage and particle internalization. Bacterial membranes and cell walls are typically of negative total charge. Electrostatic attractions can occur between bacterial surfaces and metal oxide nanoparticles of positive zeta potential [7, 55, 56]. The PZC results of samples (seen in Figure 5) showed that CuO is doped into ZnO; the PZC of material is also increased that leads to increasing of positive ions then enhancing the antibacterial effect of materials.

As seen in Figure 8, shoe insole-coated CuO-ZnO nanocomposite (CuZn/S-1 sample) had high antimicrobial activity against *S. aureus*; there are no colonies that appeared on the surface of this sample. Besides, its high

antibacterial activity can also be seen in the antibacterial width of about 3–5 mm on four edges of the shoe insoles. The antibacterial activity is reduced significantly when it is soaked and washed with soap combined with rubbing (CuZn/S-2 sample). This can be explained that the combination of washing and rubbing with soap caused CuO-ZnO attached to the surface of the CuZn/S-2 sample to be lost much more than that of the initial sample (CuZn/S-1). But that is not reduced for samples soaked in the soap solution for 24 hours (CuZn/S-3 sample).

The experimental results show that, after washing 1 time with both soaking and rubbing and only soaking in the soap solution, the loss mass of the samples was reduced by about 3 and 1 wt.%, respectively, including CuO-ZnO nanocomposite and fabric glue. Therefore, the surface morphology of the samples is almost unchanged (seen in Figure 9). And the results showed that the distribution density of nanocomposite on the surface of the CuZn/S-3 sample (Figure 9(d)) is higher than that of the CuZn/S-2 (Figure 9(c)) sample. Besides, the EDS mapping image shows that CuO-ZnO is still distributed on the surface of the sample. These results proved that CuO-ZnO nanocomposite was implanted durably on the shoe insoles.

#### 4. Conclusion

CuO-ZnO nanocomposite was successfully synthesized by the sol-gel method with the nanoparticle size in a range of 20–50 nm. It had antibacterial activity against *E. coli*, *Salmonella*, *P. aeruginosa*, *B. cereus*, and *S. aureus*. Depending on the bacteria, the value of the minimum inhibitory concentration against each bacterium is different, ranging from 0.313 to 20 mg·mL<sup>-1</sup>. CuO-ZnO nanocomposite had performed significantly higher antibacterial activity than pure ZnO nanoparticles. Furthermore, it coated on shoe insoles also with a mass percentage of 0.35 wt.% that had high antibacterial activity against *S. aureus*. These results proved that the obtained CuO-ZnO nanocomposite could be useful for the development of newer and more effective antibacterial agents for healthcare.

#### Data Availability

The data used to support the findings of this study are included within the article.

#### Conflicts of Interest

The authors declare that there is no conflict of interests regarding the publication of this paper.

#### Acknowledgments

This research was funded by the Global Challenges Research Fund (GCRF) under grant number BH192597.

#### References

- [1] J. Halfvarsson, N. Heijne, P. Ljungman, M. N. Ham, G. Holmgren, and G. Tomson, "Knowing when but not how! - mothers' perceptions and use of antibiotics in a rural area of Vietnam," *Tropical Doctor*, vol. 30, no. 1, pp. 6–10, 2000.
- [2] V. Gandhi, R. Ganesan, H. H. Abdulrahman Syedahamed, and M. Thaiyan, "Effect of cobalt doping on structural, optical, and magnetic properties of ZnO nanoparticles synthesized by coprecipitation method," *The Journal of Physical Chemistry C*, vol. 118, no. 18, pp. 9715–9725, 2014.
- [3] J. Li, H. Sang, H. Guo et al., "Antifungal mechanisms of ZnO and Ag nanoparticles to *Sclerotinia homoeocarpa*," *Nanotechnology*, vol. 28, no. 15, article 155101, 2017.
- [4] X. Chen, S. Ku, J. A. Weibel et al., "Enhanced antimicrobial efficacy of bimetallic porous CuO microspheres decorated with Ag nanoparticles," *ACS Applied Materials & Interfaces*, vol. 9, no. 45, pp. 39165–39173, 2017.
- [5] A. K. Chatterjee, R. Chakraborty, and T. Basu, "Mechanism of antibacterial activity of copper nanoparticles," *Nanotechnology*, vol. 25, no. 13, article 135101, 2014.
- [6] T.-D. Pham and B.-K. Lee, "Cu doped TiO<sub>2</sub>/GF for photocatalytic disinfection of *Escherichia coli* in bioaerosols under visible light irradiation: application and mechanism," *Applied Surface Science*, vol. 296, pp. 15–23, 2014.
- [7] J. Li, Z. Wu, Y. Bao et al., "Wet chemical synthesis of ZnO nanocoating on the surface of bamboo timber with improved mould-resistance," *Journal of Saudi Chemical Society*, vol. 21, no. 8, pp. 920–928, 2017.
- [8] N. Haghighi, Y. Abdi, and F. Haghighi, "Light-induced antifungal activity of TiO<sub>2</sub> nanoparticles/ZnO nanowires," *Applied Surface Science*, vol. 257, no. 23, pp. 10096–10100, 2011.
- [9] I. Chauhan, S. Aggrawal, and P. Mohanty, "ZnO nanowire-immobilized paper matrices for visible light-induced antibacterial activity against *Escherichia coli*," *Environmental Science: Nano*, vol. 2, no. 3, pp. 273–279, 2015.
- [10] J. Li, H. Yu, Z. Wu et al., "Room temperature synthesis of crystalline anatase TiO<sub>2</sub> on bamboo timber surface and their short-term antifungal capability under natural weather conditions," *Colloids and Surfaces A: Physicochemical and Engineering Aspects*, vol. 508, pp. 117–123, 2016.
- [11] Y.-H. Hsueh, K.-S. Lin, W.-J. Ke et al., "The antimicrobial properties of silver nanoparticles in *Bacillus subtilis* are mediated by released Ag<sup>+</sup> ions," *PloS one*, vol. 10, no. 12, article e0144306, 2015.
- [12] Z. Lu, C. Mao, M. Meng et al., "Fabrication of CeO<sub>2</sub> nanoparticle-modified silk for UV protection and antibacterial applications," *Journal of Colloid and Interface Science*, vol. 435, pp. 8–14, 2014.
- [13] H. Negi, T. Agarwal, M. Zaidi, and R. Goel, "Comparative antibacterial efficacy of metal oxide nanoparticles against Gram negative bacteria," *Annals of Microbiology*, vol. 62, no. 2, pp. 765–772, 2012.
- [14] J. A. Mary, J. J. Vijaya, L. J. Kennedy, and M. Bououdina, "Microwave-assisted synthesis, characterization and antibacterial properties of Ce-Cu dual doped ZnO nanostructures," *Optik*, vol. 127, no. 4, pp. 2360–2365, 2016.
- [15] S. Senthilkumar and T. Sivakumar, "Green tea (*Camellia sinensis*) mediated synthesis of zinc oxide (ZnO) nanoparticles and studies on their antimicrobial activities," *International Journal of Pharmacy and Pharmaceutical Sciences*, vol. 6, no. 6, pp. 461–465, 2014.
- [16] G. Y. Nigussie, G. M. Tesfamariam, B. M. Tegegne et al., "Antibacterial activity of Ag-doped TiO<sub>2</sub> and Ag-doped ZnO



- nanoparticles,” *International Journal of Photoenergy*, vol. 2018, Article ID 5927485, 7 pages, 2018.
- [17] M. Arshad, A. Azam, A. S. Ahmed, S. Mollah, and A. H. Naqvi, “Effect of Co substitution on the structural and optical properties of ZnO nanoparticles synthesized by sol–gel route,” *Journal of Alloys and Compounds*, vol. 509, no. 33, pp. 8378–8381, 2011.
  - [18] Y. Liu, H. Liu, Z. Chen et al., “Effects of Ni concentration on structural, magnetic and optical properties of Ni-doped ZnO nanoparticles,” *Journal of Alloys and Compounds*, vol. 604, pp. 281–285, 2014.
  - [19] T. K. Pathak, R. Kroon, V. Craciun, M. Popa, M. Chifiriuc, and H. Swart, “Influence of Ag, Au and Pd noble metals doping on structural, optical and antimicrobial properties of zinc oxide and titanium dioxide nanomaterials,” *Heliyon*, vol. 5, no. 3, article e01333, 2019.
  - [20] P. Amornpitoksuk, S. Suwanboon, S. Sangkanu, A. Sukhoom, N. Muensit, and J. Baltrusaitis, “Synthesis, characterization, photocatalytic and antibacterial activities of Ag-doped ZnO powders modified with a diblock copolymer,” *Powder Technology*, vol. 219, pp. 158–164, 2012.
  - [21] Y. Mao, T.-J. Park, and S. S. Wong, “Synthesis of classes of ternary metal oxide nanostructures,” *Chemical Communications*, vol. 46, pp. 5721–5735, 2005.
  - [22] I. A. Hassan, S. Sathasivam, S. P. Nair, and C. J. Carmalt, “Antimicrobial properties of copper-doped ZnO coatings under darkness and white light illumination,” *ACS Omega*, vol. 2, no. 8, pp. 4556–4562, 2017.
  - [23] C. E. Santo, P. V. Morais, and G. Grass, “Isolation and characterization of bacteria resistant to metallic copper surfaces,” *Applied and environmental microbiology*, vol. 76, no. 5, pp. 1341–1348, 2010.
  - [24] M. Ferhat, A. Zaoui, and R. Ahuja, “Magnetism and band gap narrowing in Cu-doped ZnO,” *Applied Physics Letters*, vol. 94, no. 14, article 142502, 2009.
  - [25] R. Dadi, R. Azouani, M. Traore, C. Mielcarek, and A. Kanaev, “Antibacterial activity of ZnO and CuO nanoparticles against gram positive and gram negative strains,” *Materials Science and Engineering: C*, vol. 104, p. 109968, 2019.
  - [26] E. Malka, I. Perelshtein, A. Lipovsky et al., “Eradication of multi-drug resistant bacteria by a novel Zn-doped CuO nanocomposite,” *Small*, vol. 9, no. 23, pp. 4069–4076, 2013.
  - [27] S. Preethi, K. Abarna, M. Nithyasri et al., “Synthesis and characterization of chitosan/zinc oxide nanocomposite for antibacterial activity onto cotton fabrics and dye degradation applications,” *International Journal of Biological Macromolecules*, vol. 164, pp. 2779–2787, 2020.
  - [28] S. Sathiyavimal, S. Vasantharaj, D. Bharathi et al., “Biogenesis of copper oxide nanoparticles (CuONPs) using *Sida acuta* and their incorporation over cotton fabrics to prevent the pathogenicity of Gram negative and Gram positive bacteria,” *Journal of Photochemistry and Photobiology B: Biology*, vol. 188, pp. 126–134, 2018.
  - [29] D. Bharathi, R. Ranjithkumar, B. Chandarshekar, and V. Bhuvaneshwari, “Preparation of chitosan coated zinc oxide nanocomposite for enhanced antibacterial and photocatalytic activity: as a bionanocomposite,” *International journal of biological macromolecules*, vol. 129, pp. 989–996, 2019.
  - [30] D. Bharathi and V. Bhuvaneshwari, “Synthesis of zinc oxide nanoparticles (ZnO NPs) using pure bioflavonoid rutin and their biomedical applications: antibacterial, antioxidant and cytotoxic activities,” *Research on Chemical Intermediates*, vol. 45, no. 4, pp. 2065–2078, 2019.
  - [31] K. W. Yee, *Chemical synthesis and characterization of copper coated insoles for antibacterial application*, Final Year Project (Bachelor), Tunku Abdul Rahman University College, 2018.
  - [32] J. Yip, L. Liu, K. H. Wong, P. H. Leung, C. W. M. Yuen, and M. C. Cheung, “Investigation of antifungal and antibacterial effects of fabric padded with highly stable selenium nanoparticles,” *Journal of applied polymer science*, vol. 131, no. 17, 2014.
  - [33] N. Cuesta Garrote, M. Sánchez Navarro, F. Arán Aís, and C. Orgilés Barceló, “Natural antimicrobial agents against the microbiota associated with insoles,” *Science And Technology Against Microbial Pathogens: Research, Development and Evaluation*, vol. 2011, pp. 109–113, 2011.
  - [34] D. Lu, X. Guo, Y. Li, B. Zheng, and J. Zhang, “Insoles treated with bacteria-killing nanotechnology bio-kil reduce bacterial burden in diabetic patients and healthy controls,” *Journal of Diabetes Research*, vol. 2018, Article ID 7678310, 6 pages, 2018.
  - [35] S. Azimi, “Sol-gel synthesis and structural characterization of nano-thiamine hydrochloride structure,” *ISRN Nanotechnology*, vol. 2013, Article ID 815071, 4 pages, 2013.
  - [36] R. M. Allaf and L. J. Hope-Weeks, “Synthesis of ZnO-CuO nanocomposite aerogels by the sol-gel route,” *Journal of Nanomaterials*, vol. 2014, Article ID 491817, 9 pages, 2014.
  - [37] E. N. Bakatula, D. Richard, C. M. Neculita, and G. J. Zagury, “Determination of point of zero charge of natural organic materials,” *Environmental Science and Pollution Research*, vol. 25, no. 8, pp. 7823–7833, 2018.
  - [38] P. Wayne, “Performance standards for antimicrobial susceptibility testing: 23rd informational supplement (M100-S23) CLSI,” *Clinical and Laboratory Standards Institute (CLSI)*, vol. M100-S23, 2013.
  - [39] J. Washington and G. Wood, “Antimicrobial susceptibility tests: dilution and disc diffusion methods,” *Manual of Clinical Microbiology*, vol. 1995, pp. 1327–1331, 1995.
  - [40] L. Zhu, H. Li, Z. Liu, P. Xia, Y. Xie, and D. Xiong, “Synthesis of the 0D/3D CuO/ZnO heterojunction with enhanced photocatalytic activity,” *The Journal of Physical Chemistry C*, vol. 122, no. 17, pp. 9531–9539, 2018.
  - [41] A. Patterson, “The Scherrer formula for X-ray particle size determination,” *Physical Review*, vol. 56, no. 10, p. 978, 1939.
  - [42] S. Khan, S. Shahid, S. Jabin, S. Zaman, and M. Sarwar, “Synthesis and characterization of un-doped and copperdoped zinc oxide nanoparticles for their optical and antibacterial studies,” *Digest Journal of Nanomaterials & Biostructures*, vol. 13, no. 1, pp. 285–297, 2018.
  - [43] A. Sirelkhatim, S. Mahmud, A. Seeni et al., “Review on zinc oxide nanoparticles: antibacterial activity and toxicity mechanism,” *Nano-Micro Letters*, vol. 7, no. 3, pp. 219–242, 2015.
  - [44] G. N. S. Vijayakumar, S. Devashankar, M. Rathnakumari, and P. Sureshkumar, “Synthesis of electrospun ZnO/CuO nanocomposite fibers and their dielectric and non-linear optic studies,” *Journal of Alloys and Compounds*, vol. 507, no. 1, pp. 225–229, 2010.
  - [45] H. Gómez-Pozos, E. Arredondo, A. Maldonado Álvarez et al., “Cu-doped ZnO thin films deposited by a sol-gel process using two copper precursors: gas-sensing performance in a propane atmosphere,” *Materials*, vol. 9, no. 2, p. 87, 2016.



- [46] R. Udayabhaskar and B. Karthikeyan, "Optical and phonon properties of ZnO: CuO mixed nanocomposite," *Journal of Applied Physics*, vol. 115, no. 15, article 154303, 2014.
- [47] N. Oroujzadeh, E. Delpazir, and Z. Shariatnia, "Studying the effect of particle size on the antibacterial activity of some N-nicotinyl phosphoric triamides," *Particulate Science and Technology*, vol. 37, no. 4, pp. 423–429, 2019.
- [48] O. Yamamoto, "Influence of particle size on the antibacterial activity of zinc oxide," *International Journal of Inorganic Materials*, vol. 3, no. 7, pp. 643–646, 2001.
- [49] S. R. Alharbi, M. Alhassan, O. Jalled, S. Wageh, and A. Saeed, "Structural characterizations and electrical conduction mechanism of  $\text{CaBi}_2\text{Nb}_2\text{O}_9$  single-phase nanocrystallites synthesized via sucrose-assisted sol-gel combustion method," *Journal of Materials Science*, vol. 53, no. 16, pp. 11584–11594, 2018.
- [50] G. Panzner, B. Egert, and H. P. Schmidt, "The stability of CuO and  $\text{Cu}_2\text{O}$  surfaces during argon sputtering studied by XPS and AES," *Surface Science*, vol. 151, no. 2-3, pp. 400–408, 1985.
- [51] G. Dong, B. Du, L. Liu et al., "Synthesis and their enhanced photoelectrochemical performance of ZnO nanoparticle-loaded CuO dandelion heterostructures under solar light," *Applied Surface Science*, vol. 399, pp. 86–94, 2017.
- [52] M. Kooti and A. Naghdi Sedeh, "Microwave-assisted combustion synthesis of ZnO nanoparticles," *Journal of Chemistry*, vol. 2013, Article ID 562028, 4 pages, 2012.
- [53] A. Lozhkomoev, O. Bakina, A. Pervikov, S. Kazantsev, and E. Glazkova, "Synthesis of CuO–ZnO composite nanoparticles by electrical explosion of wires and their antibacterial activities," *Journal of Materials Science: Materials in Electronics*, vol. 30, pp. 13209–13216, 2019.
- [54] N. Widiarti, J. Sae, and S. Wahyuni, "Synthesis CuO–ZnO nanocomposite and its application as an antibacterial agent," *IOP Conference Series: Materials Science and Engineering*, vol. 172, article 012036, 2017.
- [55] S. Stankic, S. Suman, F. Haque, and J. Vidic, "Pure and multi metal oxide nanoparticles: synthesis, antibacterial and cytotoxic properties," *Journal of Nanobiotechnology*, vol. 14, no. 1, article 73, 2016.
- [56] M. J. Hajipour, K. M. Fromm, A. A. Ashkarran et al., "Antibacterial properties of nanoparticles," *Trends in biotechnology*, vol. 30, no. 10, pp. 499–511, 2012.
- [57] B. Fahmy and S. A. Cormier, "Copper oxide nanoparticles induce oxidative stress and cytotoxicity in airway epithelial cells," *Toxicology In Vitro*, vol. 23, no. 7, pp. 1365–1371, 2009.
- [58] A. Lipovsky, Y. Nitzan, A. Gedanken, and R. Lubart, "Antifungal activity of ZnO nanoparticles - the role of ROS mediated cell injury," *Nanotechnology*, vol. 22, no. 10, article 105101, 2011.
- [59] Z. Huang, X. Zheng, D. Yan et al., "Toxicological effect of ZnO nanoparticles based on bacteria," *Langmuir*, vol. 24, no. 8, pp. 4140–4144, 2008.
- [60] T. Xia, M. Kovochich, M. Liong et al., "Comparison of the mechanism of toxicity of zinc oxide and cerium oxide nanoparticles based on dissolution and oxidative stress properties," *ACS Nano*, vol. 2, no. 10, pp. 2121–2134, 2008.
- [61] J. Kiwi and V. Nadtochenko, "Evidence for the mechanism of photocatalytic degradation of the bacterial wall membrane at the  $\text{TiO}_2$  interface by ATR-FTIR and laser kinetic spectroscopy," *Langmuir*, vol. 21, no. 10, pp. 4631–4641, 2005.
- [62] J. Sawai, "Quantitative evaluation of antibacterial activities of metallic oxide powders (ZnO, MgO and CaO) by conductimetric assay," *Journal of microbiological Methods*, vol. 54, no. 2, pp. 177–182, 2003.
- [63] V. Lakshmi Prasanna and R. Vijayaraghavan, "Insight into the mechanism of antibacterial activity of ZnO: surface defects mediated reactive oxygen species even in the dark," *Langmuir*, vol. 31, no. 33, pp. 9155–9162, 2015.
- [64] K. Hirota, M. Sugimoto, M. Kato, K. Tsukagoshi, T. Tanigawa, and H. Sugimoto, "Preparation of zinc oxide ceramics with a sustainable antibacterial activity under dark conditions," *Ceramics International*, vol. 36, no. 2, pp. 497–506, 2010.